

Phonon-induced conductivity of ballistic quantum wires

A. J. Kent, A. J. Naylor, P. Hawker, and M. Henini

School of Physics and Astronomy, University of Nottingham, University Park, Nottingham NG7 2RD, United Kingdom

(Received 24 April 2000)

We have used pulses of nonequilibrium phonons to probe the electron-phonon interaction in a ballistic quantum wire. Phonons incident on the wire caused a decrease in its conductance, $-\Delta G$, due to phonon-induced electron backscattering. We observed giant oscillations in $-\Delta G$ as the wire was narrowed. Maxima occurred when E_F was close to the bottom of any one-dimensional subband. An applied magnetic field broadened and shifted the phonoconductivity oscillations, due to the depopulation of the hybrid electric-magnetic subbands. When the wire was just pinched off, the phonons caused a strong increase in the conductivity due to phonon-assisted transfer of electrons across the potential barrier.

A knowledge of the carrier-phonon interaction in electronic nanostructures is essential to understand important aspects of device behavior, for example, hot carrier effects and energy relaxation. The best way to obtain detailed information about carrier-phonon scattering processes is to make direct phonon measurements, i.e., phonon emission and absorption experiments. Acoustic phonons also make ideal spectroscopic probes of such systems because their wavelength and energy are comparable to the important length and energy scales of the carrier states. The value of direct phonon measurements has already been proven in studies of two-dimensional electron systems (see, for example, Refs. 1, 2). Although considerable theoretical work on the electron-acoustic phonon interaction in quantum wires has been reported (see, for example, Refs. 3–7), there have, to our knowledge, been very few, if any, direct experimental measurements on these systems.

In an earlier paper,⁸ we described phonon absorption measurements on a 10- μm -long nonballistic quantum wire. Acoustic phonons were generated by a thin-film heater on the face of the substrate opposite the wire, and detected via the phonon-induced change in the wire conductance (phonoconductivity). The phonons caused an increase in the conductance which we attributed to the phonon-induced delocalization of weakly localized electron states. In this article, we describe measurements on a short ballistic wire (quantum point contact) using the same technique.

The quantum point contact (QPC) used in the experiments described here was formed in a GaAs/ $\text{Al}_x\text{Ga}_{1-x}\text{As}$ heterojunction by the well-established split-gate technique.⁹ The two-dimensional electron gas (2DEG) in the heterojunction had an areal density of $4.4 \times 10^{15} \text{ m}^{-2}$ and a mobility of $100 \text{ m}^2 \text{ V}^{-1} \text{ s}^{-1}$ at 4.2 K. A device, 0.5-mm-wide \times 3-mm-long, was defined by a conventional wet etch and ohmic contacts were made at its ends. A split gate was fabricated in the middle of the device by electron-beam lithography, the gate separation at the point contact was 400 nm. On the polished face of the GaAs wafer opposite the device, a 100- μm -long \times 10- μm -wide, 50- Ω CuNi heater was fabricated photolithographically. Infrared front-to-back alignment was used to place the heater directly opposite the point contact, with the heater's long axis aligned perpendicular to the channel.

Ballistic nonequilibrium phonons were generated by applying short ($\approx 20 \text{ ns}$) electrical pulses to the heater. The heater temperature, T_h , could be determined by acoustic mismatch calculations,¹⁰ and the peak in the Planckian spectrum of generated phonons was at frequency $2.8k_B T_h/h$. The electron-phonon interaction was measured by the phonoconductivity, i.e., the transient change in conductance of the device caused by the incident phonon pulse. A constant bias current of 100 nA was passed through the device and the small ($\sim \mu\text{V}$) voltage changes detected by a high-speed digitizer and signal averager. A detailed description of the experimental method, including a discussion of the methods used to minimize electromagnetic breakthrough and other spurious responses, is given in Ref. 8. Figure 1 shows the device response to the incident phonons as a function of time after the heater pulse. The split gate bias, V_G , was -1.7 V and $T_h = 28 \text{ K}$. After about 80 ns, which is the time taken for ballistic longitudinal (LA) phonons ($v_{TL} \approx 5000 \text{ m s}^{-1}$) to traverse the GaAs substrate, the initial sharp rise of the signal is seen. Another sharp increase is seen 120 ns after the pulse. This is due to ballistic transverse (TA) phonons ($v_{TA} \approx 3300 \text{ m s}^{-1}$) reaching the device. The signal continues to rise while phonons are incident on the QPC. After the peak, the signal decays away slowly due to the long electrical time

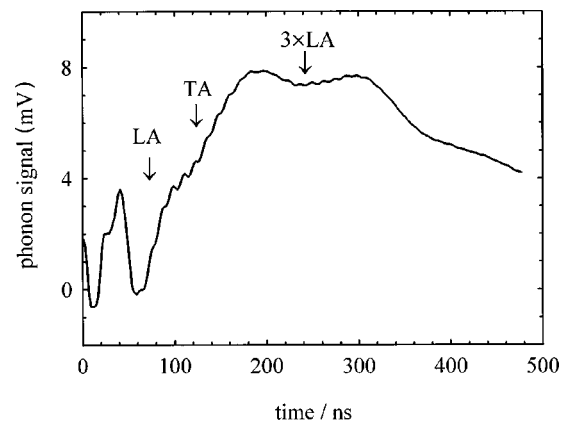


FIG. 1. Time dependence of phonon-induced conductivity. The start of the heater excitation pulse is at $t=0$ and the features between 0 and 50 ns are due to residual electromagnetic breakthrough. The arrows show the arrival times of the ballistic phonon modes.

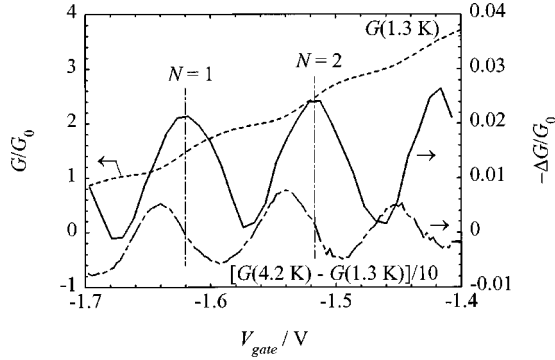


FIG. 2. Strength of phonoconductivity response as a function of the gate bias voltage. Also shown is the dc conductance at $T = 1.3$ K and the difference between the dc conductance at 1.3 and 4.2 K. G_0 is the conductance quantum ($= 2e^2/h$).

constant of the measuring system ($RC \approx 0.5 \mu\text{s}$). The secondary peak starting about 240 ns after the pulse is due to phonons reflected off the top and bottom surfaces of the substrate, traversing the thickness of the wafer two more times before falling on the device again. Observation of the ballistic phonon peaks in the time-resolved trace allows us to differentiate between the device's response to ballistic phonons and to any heating of the entire sample by the phonon pulse. The polarity of the phonoconductivity is negative, i.e., the phonon pulse causes a transient decrease in conductance of the QPC. We checked that the signal was not due to thermoelectric effects by removing the bias current, upon which any trace of the signal disappeared.

Figure 2 shows the strength of the phonoconductivity as a function of V_G . This was obtained by integrating the signal shown in Fig. 1 over 80–180 ns (the time interval during which the phonon signal was increasing). Oscillations are observed with an amplitude $|\Delta G/G_0| \approx 2\%$ and with ΔG dropping near to zero between the peaks. Closer examination reveals that the phonoconductivity maxima occur near to steps in the dc conductance of the point contact. Before proceeding to discuss these measurements in relation to the current theories of electron-phonon interactions in quantum wires, it is important to consider the possible heating effects of the phonon pulse. Heating of the entire sample was measured using superconducting transition edge bolometers. We found that the sample, which was immersed in liquid helium II at $T = 1.3$ K, warmed by just a few tens of mK during a pulse and cooled on a sub- μs timescale (faster than the pulse repetition period). Heating of the 2D electron system by phonon absorption was measured without gate bias. By measuring the change of resistance of the 2DEG induced by the phonon pulses and comparing this with a calibration of steady-state resistance vs temperature, we estimate the 2DEG temperature is raised about 1 K in the area directly opposite the heater. Also shown in Fig. 2 is the effect on the conductivity of heating the sample by approximately 3 K (larger than both the above values). This was obtained by subtraction of dc conductance measurements at 1.3 K and 4.2 K. The heating effect clearly differs from the phonoconductivity in two distinct ways: first, the heating oscillates symmetrically about zero conductance change and, secondly, the phase of the oscillations is different. We therefore attribute the observed phonoconductivity to direct electron-phonon

scattering with heating only playing a very minor role.

Increasing the (negative) gate bias narrows the point contact and so increases the separation of the quasi-one-dimensional (1D) electronic subbands in the channel. The 1D density of states (DOS) at the Fermi energy, E_F , is sharply peaked when the bottom of the N th 1D band at E_N coincides with E_F (E_F is assumed constant at the value of the 2D reservoirs since $eV_{ch} \ll E_F$, where V_{ch} is the voltage drop across the 1D channel). Therefore, the dc conductivity, which is proportional to the integral of the DOS, exhibits step-wise behavior.⁹ On the other hand, the probability of phonon scattering is proportional to the DOS and so the phonoconductivity exhibits oscillations. For $|\Delta G| \ll G_0$, the size of the conductance change is given by $\Delta G/G_0 \approx -\tau/\tau_B$, where τ is the time an electron takes to propagate through the wire and τ_B^{-1} is the backscattering rate. Assuming the effective channel length $L_y \sim 200$ nm (allowing for reasonable ‘‘rounding’’ of the gate points), we obtain $\tau_B^{-1} \sim \{2(E_F - E_N)/m^*L_y\}^{1/2} \Delta G/G_0 \approx 0.4 \text{ ns}^{-1}$ for $(E_F - E_N) \approx k_B T$.

For an ideal ballistic quantum wire that shows well-defined quantized conductance steps, phonon emission and absorption are expected to lead to backscattering of electrons, and so a decrease in conductance. Gurevich *et al.*⁶ used the kinetic equation approach to calculate the change in conductance due to scattering by equilibrium phonons. They found that the phonon-assisted conductance is negative because of backscattering and it oscillates due to quantum size effects, as discussed above. The peaks in the oscillations occur close to the 1D band edge owing to the divergence of the 1D density of states. Blencowe and Shik⁷ consider the case of backscattering by nonequilibrium phonons, which is more relevant to our experiment. They arrive at an expression for ΔG which takes the following form (for deformation potential coupling):

$$\Delta G = -\frac{e^2 L_y m^* \Xi^2}{8\pi\hbar^2 \rho v_s} \sum_{MN} \frac{1}{\sqrt{E_F - E_N}} \times \int dq_x \int dq_z \frac{q N_q |Z(q_z)|^2 |X(q_x)|^2}{\sqrt{E_F - E_M + \hbar\omega_q}}, \quad (1)$$

where Ξ is the deformation potential constant; q is the phonon wave vector and $\hbar\omega_q$ its energy; N_q is the phonon (Bose) distribution function; ρ is the crystal density and v_s the phonon velocity; the confined state ‘‘form factors’’ $|Z(q_z)|^2$ and $|X(q_x)|^2$ account for momentum nonconservation in the x and z directions (perpendicular to the wire); and the other symbols have their usual meanings. We see from this expression that ΔG is always negative and diverges at $E_F \approx E_N$.

Our experimental observations are in broad qualitative agreement with the theoretical predictions. However, the amplitude of the conductivity oscillations estimated using Eq. (1) turns out to be one to two orders of magnitude smaller than measured.¹¹ The reason for this is that in the chosen geometry (a small heater placed directly opposite the QPC) phonons are incident close to normal to the QWR. As such, they would not appear to possess sufficiently large q_y wave vector components to cause backscattering. The fact that we

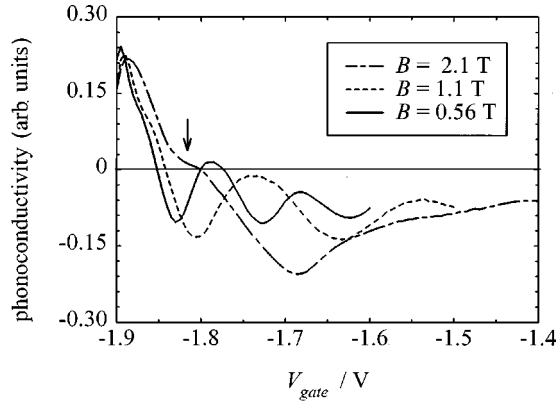


FIG. 3. Phonoconductivity as a function of gate bias at various values of the applied magnetic field.

see any signal at all is due to the acoustic anisotropy of the GaAs substrate material which leads to phonon focusing.¹² As a result, a small but a significant fraction of the incident phonons can have their wave vectors oriented at angles of up to 40° away from their energy propagation direction, and are thus able to cause backscattering when incident near normal to the QPC. These phonons are predominantly TA modes focused close to $[001]$. Including the effects of acoustic anisotropy in the calculation of the electron-phonon matrix elements is also necessary. Without it, TA phonons would not couple to the electrons by the deformation potential. It has been shown that proper consideration of acoustic anisotropy is necessary to explain the results of phonon experiments on 2D electron systems fully.¹³ However, the effects of acoustic anisotropy have not so far been fully included in the calculations for 1D electronic systems. Further theoretical work is needed to resolve this issue.

The phonoconductivity oscillations measured with a magnetic field applied parallel to z (the heterojunction growth direction) are shown in Fig. 3. Increasing the magnetic field spreads out the peaks and also shifts them to a smaller (negative) gate bias. This is due to the formation of hybridized electric-magnetic subbands.¹⁴ In an applied magnetic field, the bottoms of the 1D electronic subbands are at $E_N = (N + \frac{1}{2})\hbar\omega$, where $\omega = (\omega_0^2 + \omega_c^2)^{1/2}$. Here, ω_0 is the characteristic frequency of the harmonic oscillator wave functions due to the electric confinement (this assumes the electric confining potential along the x direction is parabolic in shape) and ω_c is the cyclotron frequency ($\omega_c = eB/m^*$). The energy separation of the subbands is now increased compared to the zero field situation. If we follow the phonoconductance peak due to a particular subband, labeled M , increasing the magnetic field (and so ω_c), requires a reduction in ω_0 to maintain $E_M = E_F$. This means the electric confinement must be reduced and the peak moves to smaller gate bias, as observed.

Another effect of the applied magnetic field is to increase the dynamical effective mass of the 1D electrons by a factor ω^2/ω_0^2 , i.e., $m^*(B) = m^*(0)\{1 + \omega_c^2/\omega_0^2\}$.¹⁴ This can be understood semiclassically by picturing the electrons under the influence of the magnetic field as performing ‘‘skipping orbits’’ along the walls of the 1D channel. The result is that the group velocity of the electrons through the channel is reduced and this may be accounted for by a correction to the effective mass. The strength of the phonoconductivity is pro-

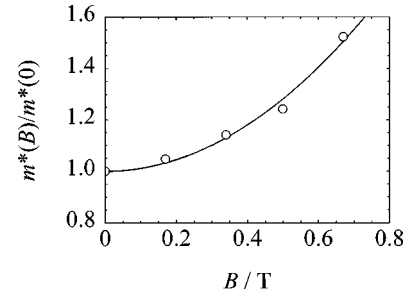


FIG. 4. Amplitude of the phonoconductivity oscillations as a function of applied magnetic field B normalized to the amplitude at $B=0$. The solid line is from $m^*(B)/m^*(0) = (1 + \omega_c^2/\omega_0^2)$.

portional to m^* [Eq. (1)] hence the observation of an increase in amplitude of the phonoconductivity oscillations with increasing magnetic field. Figure 4 shows the amplitude of the phonoconductivity oscillations (normalized to zero magnetic field) as a function of the applied magnetic field strength. The solid line is given by $m^*(B) = m^*(0)\{1 + \omega_c^2/\omega_0^2\}$ fitted to the data points. From the fitting parameters we obtain $\omega_0 = 2.4 \times 10^{12} \text{ s}^{-1}$ which gives an effective wire width $l_w = (\hbar/m^*\omega_0)^{1/2} = 26 \text{ nm}$ at the $N=0$ step. This value is consistent with that obtained from conventional magnetotransport measurements on the same sample.

At fields above 2 T, an additional phonoconductance peak develops beyond the $N=0$ maximum. This peak is shown by the arrow in Fig. 3. It appears to coincide with a weak step at e^2/h in the dc conductance data and is probably due to a lifting of the spin degeneracy of the subband. It is interesting that as the field is reduced to zero, this feature does not completely disappear, but persists as a weak ledge on the side of the $N=0$ peak. This phenomenon may have the same origins as the step at $0.7(2e^2/h)$ observed in transport measurements.¹⁵ It is believed this feature may be due to electron-electron interactions.

Turning our attention now to higher gate voltages where the device is pinched off, we notice that the phonoconductivity changes sign (the peak at $V_{\text{gate}} \approx -1.9 \text{ V}$ in Fig. 3). That is the incident phonons caused a strong increase in the device conductance. It was again checked that the positive photoconductivity was not due to heating. In the pinch off regime, the signal appeared to show activated behavior with

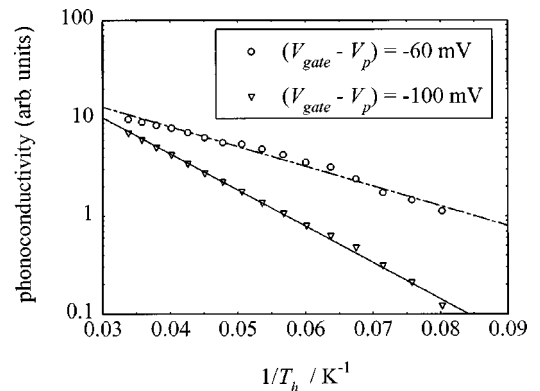


FIG. 5. Strength of phonoconductivity response at pinch off as a function of the phonon source (heater) temperature. V_p is the gate voltage at the $N=0$ dc conductance step.

respect to T_h , see Fig. 5. This suggests that we were observing phonon-assisted transfer of electrons across the potential barrier at the QPC. Under these conditions the signal should be proportional to the number of phonons in the heater spectrum of energy equal to an activation gap Δ . For $\Delta \gg k_B T_h$, the phonon occupation number at an energy Δ is proportional to $\exp(-\Delta/k_B T_h)$ and so Δ can be extracted from an Arrhenius plot. Defining V_p as the gate voltage of the $N=0$ conductance step, then for an offset of $(V_{\text{gate}} - V_p) = -60$ mV, $\Delta = 4$ meV. This increases to 7 meV for an offset of -100 mV. Interestingly, the ratio of the activation energies (≈ 1.7) is very nearly the same as the ratio of voltage offset. We propose that, because of phonon absorption, an electron in the 2DEG source contact is promoted into the empty $N=0$ subband upon which it contributes to the conduction. Although the absorption of meV phonons by a GaAs 2DEG is expected to be very weak due to momentum conservation selection rules, it is only necessary to excite a few electrons to cause a significant fractional conductance change in the pinch off regime. It is possible that after calibration, such a point-contact device could be used as a tunable phonon de-

tector.

In summary, we have studied the phonon-induced conductivity of a ballistic quantum point contact device. We identified two contributions to the signal: (i) direct phonon-induced backscattering of electrons in the QPC, and (ii) phonon-activated conduction as the channel is pinched off. We have shown that heating effects make a negligible contribution to the phonoconductivity. The characteristics of the phonoconductivity agree with theoretical predictions except the magnitude of the signal. However, we suggest that if the effects of acoustic anisotropy on the phonon distribution and the electron-phonon coupling matrix elements are included in the theory, full quantitative agreement may be obtained. Measurements of the phonoconductivity in a magnetic field show that the phonoconductivity is a sensitive probe of the electronic states in 1D systems.

The authors would like to thank Professor A. Shik, Dr. M. Blencowe, and Dr. D. Lehmann for helpful discussions. This work was supported by the Engineering and Physical Sciences Research Council of UK, under Grant No. GR/K 55561.

¹S. Roshko, W. Dietsche, and L. J. Challis, Phys. Rev. Lett. **80**, 3835 (1998).

²U. Zeitler, A. M. Devitt, J. E. Digby, C. J. Mellor, A. J. Kent, K. A. Benedict, and T. Cheng, Phys. Rev. Lett. **82**, 5333 (1999).

³U. Brockelmann and G. Bastard, Phys. Rev. B **42**, 8947 (1990).

⁴R. Mickevicius and V. Mitin, Phys. Rev. B **48**, 17 194 (1993).

⁵A. Y. Shik and L. J. Challis, Phys. Rev. B **47**, 2082 (1993).

⁶V. L. Gurevich, V. B. Pevzner, and K. Hess, Phys. Rev. B **51**, 5219 (1995).

⁷M. Blencowe and A. Shik, Phys. Rev. B **54**, 13 899 (1996).

⁸A. J. Kent, A. J. Naylor, P. Hawker, M. Henini, and B. Bracher, Phys. Rev. B **55**, 9775 (1997).

⁹T. J. Thornton, M. Pepper, H. Ahmed, D. Andrews, and G. J. Davies, Phys. Rev. Lett. **56**, 1198 (1986).

¹⁰W. A. Little, Can. J. Phys. **37**, 334 (1959).

¹¹M. P. Blencowe, J. Phys.: Condens. Matter **8**, 3121 (1996).

¹²J. P. Wolfe, *Imaging Phonons: Acoustic Wave Propagation in Solids* (Cambridge University Press, Cambridge, 1998).

¹³D. Lehmann, Cz Jasiukiewicz, and A. J. Kent, Physica B **249-251**, 718 (1998).

¹⁴K. F. Berggren, T. J. Thornton, D. J. Newson, and M. Pepper, Phys. Rev. Lett. **57**, 1769 (1986).

¹⁵K. J. Thomas, J. T. Nicholls, M. Y. Simmons, M. Pepper, D. R. Mace, and D. A. Ritchie, Phys. Rev. Lett. **77**, 135 (1996).